

Supporting Information

Electrochemistry and Electrogenerated Chemiluminescence of Three Phenanthrene Derivatives, Enhancement of Radical Stability and Electrogenerated Chemiluminescence Efficiency by Substituent Groups

Honglan Qi[†], Yu-Han Chen[‡], Chien-Hong Cheng[‡] and Allen J Bard^{*†}

[†]*Center for Electrochemistry, Department of Chemistry and Biochemistry, The University of Texas, Austin, Texas 78712*

[‡]*Department of Chemistry, National Tsing-Hua University, Hsinchu 30013, Taiwan*

* To whom correspondence should be addressed. E-mail: ajbard@mail.utexas.edu. Phone: (512) 471-3761; Fax (512) 471-0088.

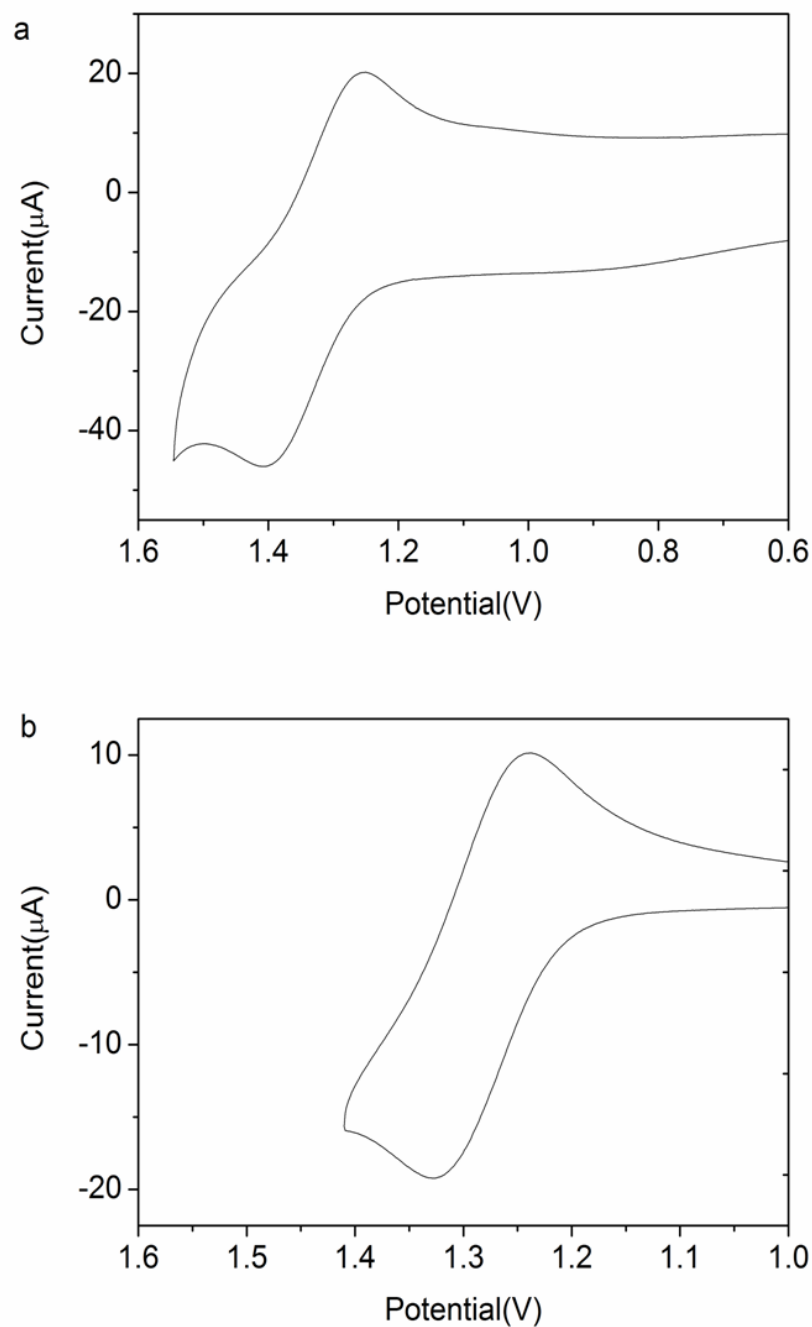


Figure S1. (a) Cyclic voltammograms of 0.5 mM TphP in MeCN/Bz ($v:v=1:1$) containing 0.1 M TBAPF₆ with a scan rate of 10 V/s; (b) cyclic voltammograms of 0.5 mM TnaP in MeCN:Bz ($v:v=1:1$) containing 0.1 M TBAPF₆ with a scan rate of 1 V/s. All scans start in the positive direction.

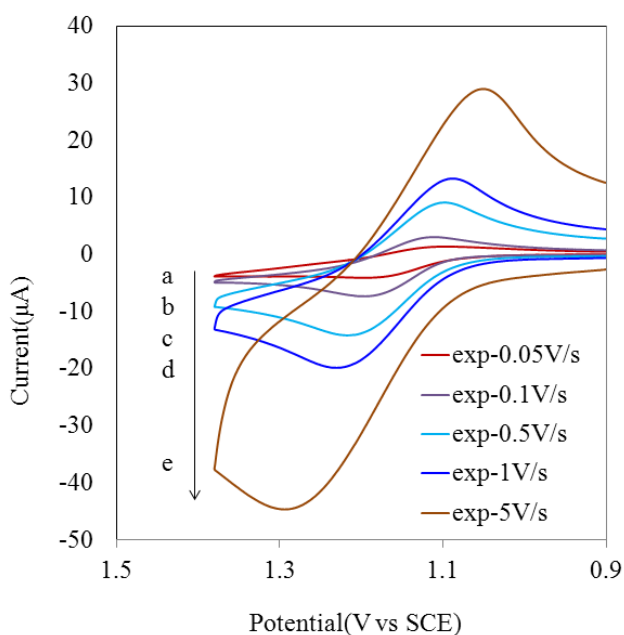
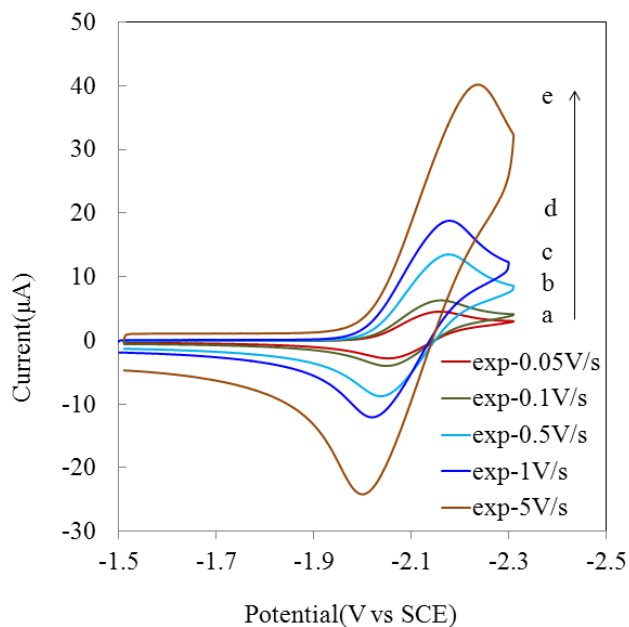


Figure S2. (Top) Reduction voltammogram of 0.8 mM TpyP in MeCN:Bz ($v:v=1:1$) at various scan rates (v). Inset: reduction peak current versus $v^{1/2}$. (Bottom) Oxidation voltammogram of 0.8 mM TpyP in MeCN:Bz ($v:v=1:1$) at various scan rates. a) 0.05 V/s; b) 0.1 V/s; c) 0.5 V/s; d) 1 V/s; e) 5 V/s.

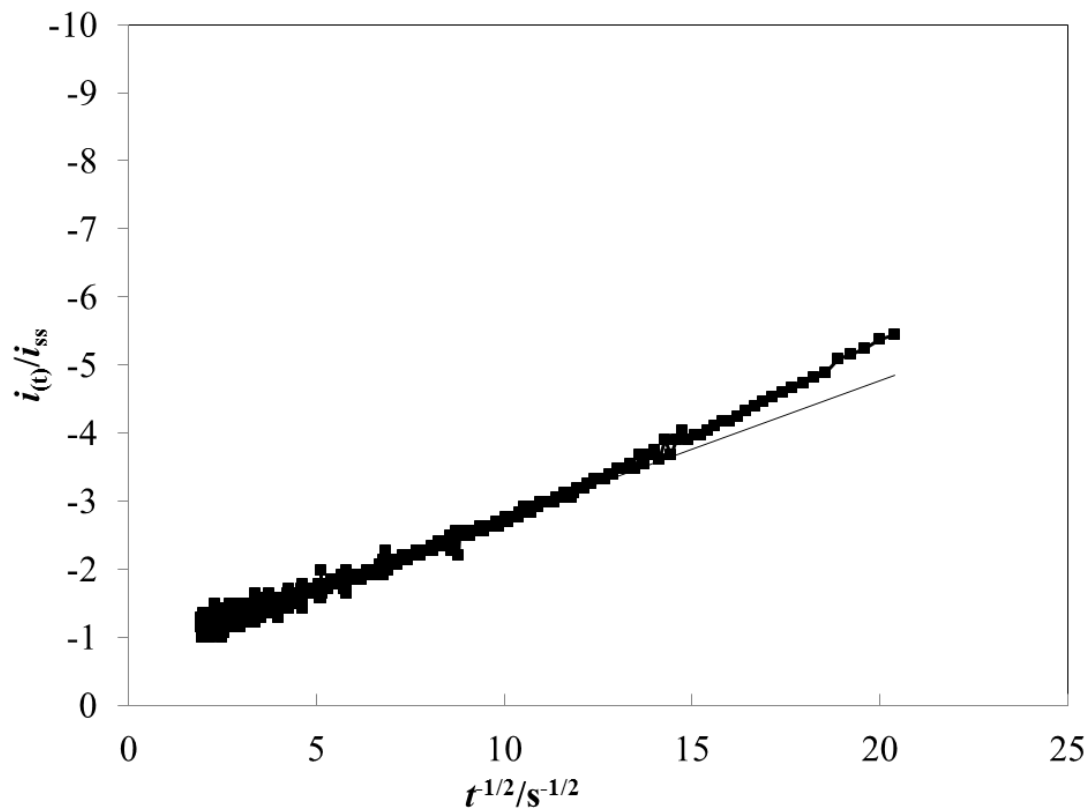


Figure S3. Plot of the experimental ratio $i_{(t)}/i_{ss}$ against the inverse square root of time of 0.5 mM TnaP in 0.1 M TBAPF₆ with 12.5 μm radius Pt UME in MeCN:Bz ($v:v=1:1$). Oxidation at step potential $E = +1.4$ V vs Ag.

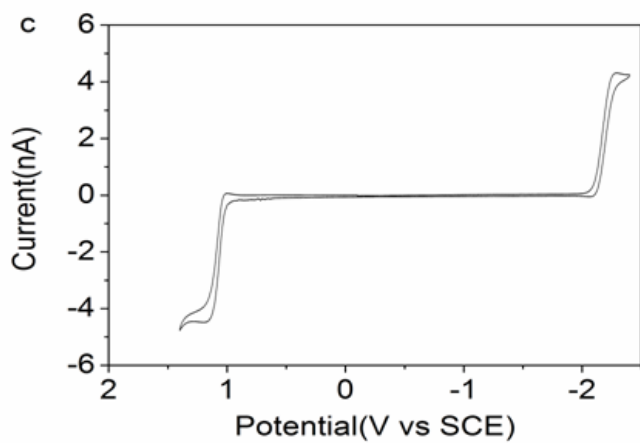
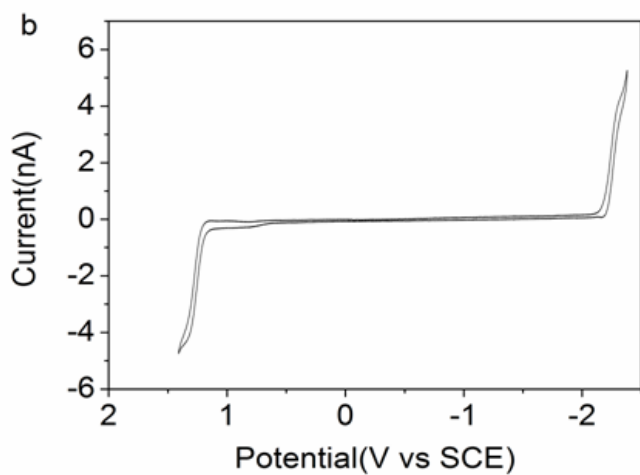
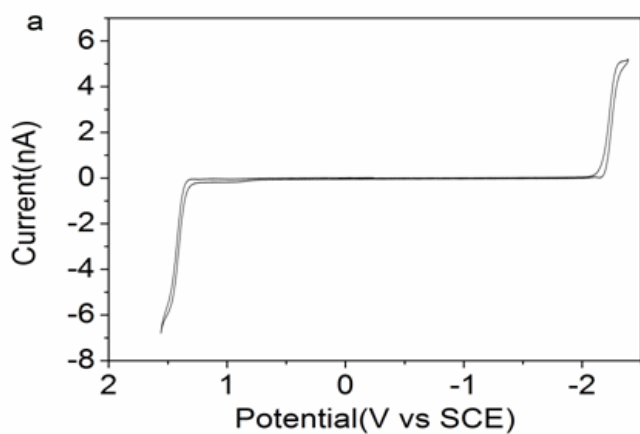


Figure S4. Cyclic voltammogram of 0.5 mM Tphp (a), 0.5 mM TnaP (b) and 0.8 mM TpyP (c) in MeCN:Bz ($v:v=1:1$) and 0.1 M TBAPF₆ on Pt UME, radius $a = 12.5 \mu\text{m}$. Scan rate = 100 mV/s. All scans start in the negative direction.

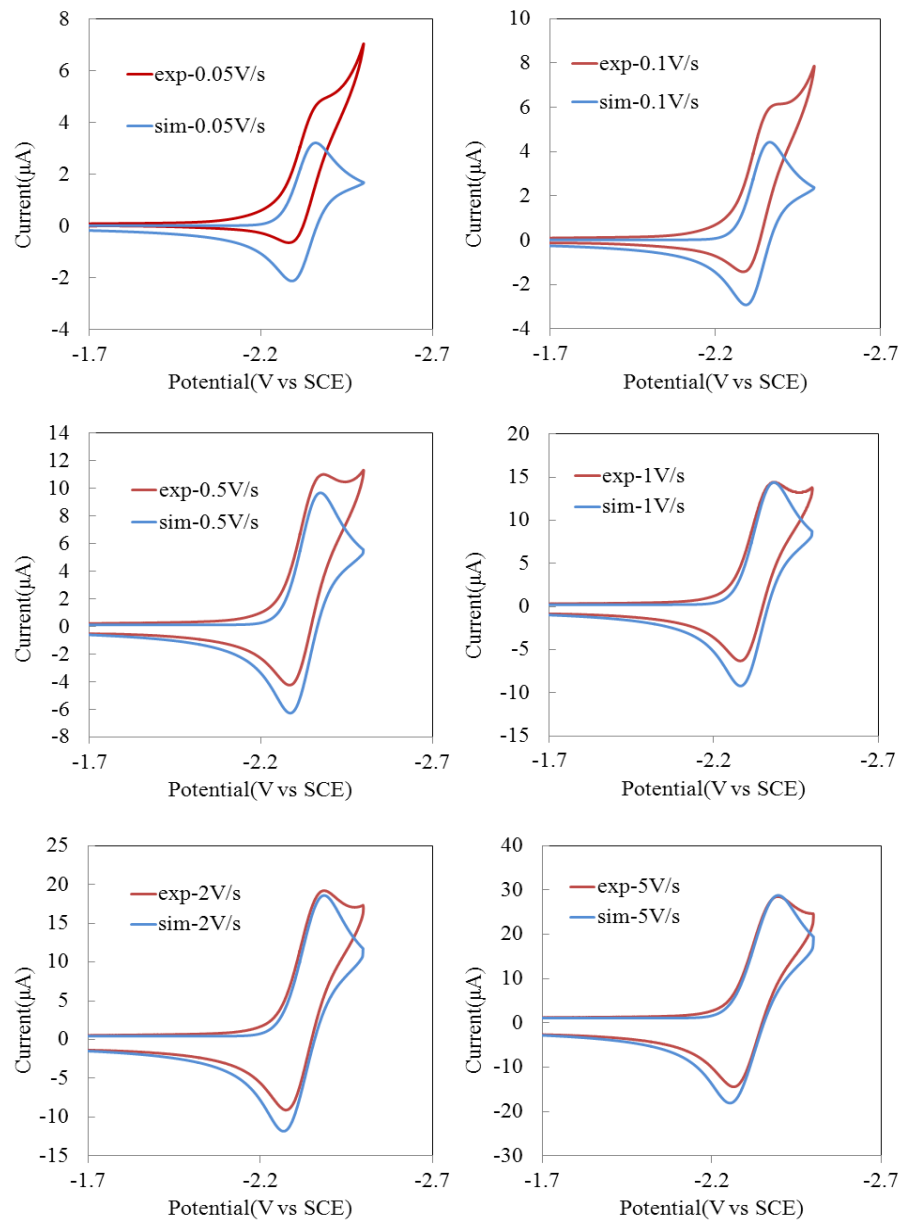


Figure S5. Experimental (red line) and simulated (blue line) cyclic voltammograms of 0.5 mM TphP reduction. The model for these simulations was E, with $n = 1$, uncompensated resistance $\sim 442 \Omega$, $C_{dl} = 2.2 \times 10^{-7} \text{ F}$, $E^0 = -2.33 \text{ V vs. SCE}$, $k^0 = 0.025 \text{ cm/s}$, $\alpha = 0.5$, $D = 6.69 \times 10^{-6} \text{ cm}^2$.

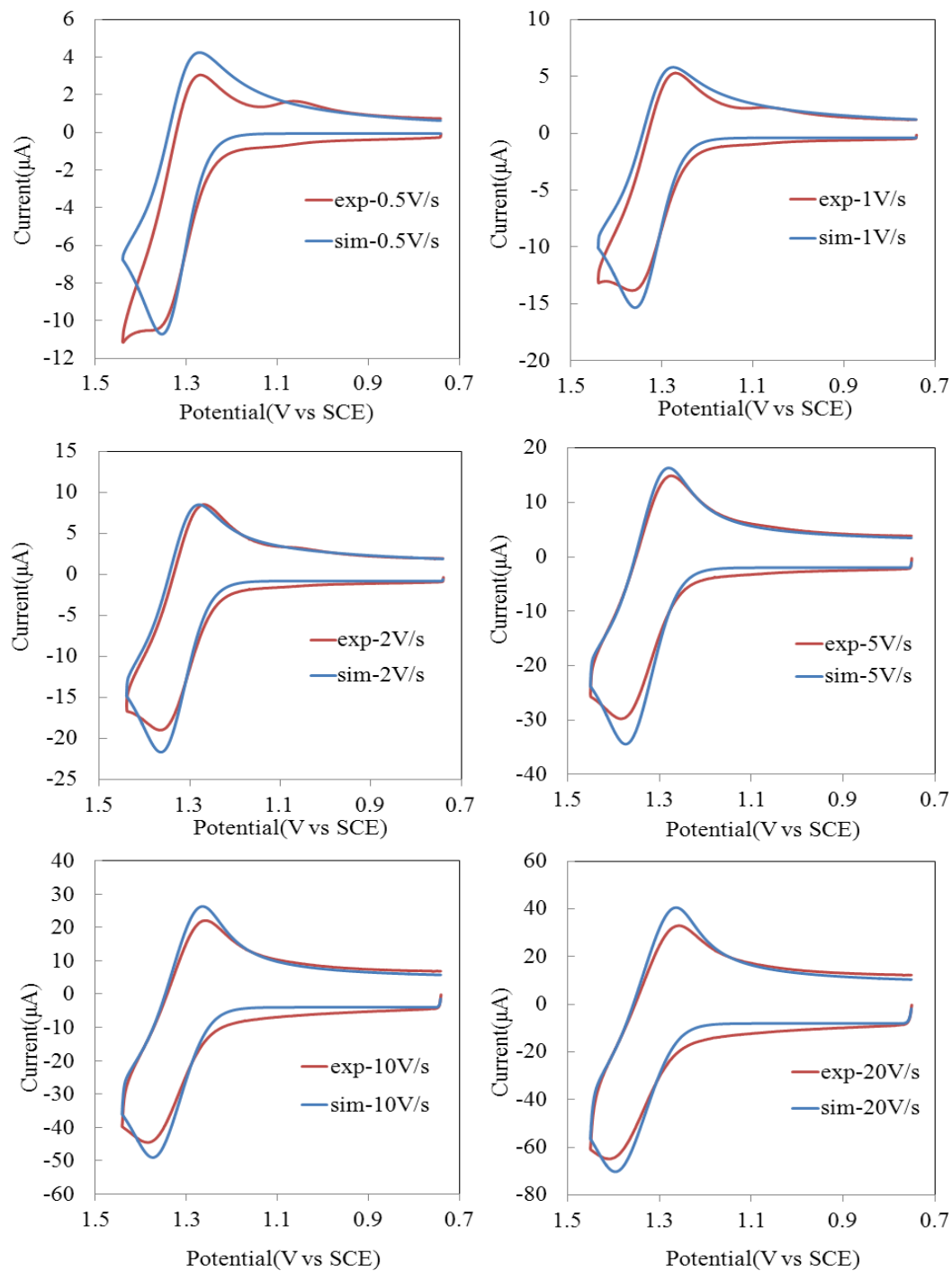


Figure S6. Experimental (red line) and simulated (blue line) cyclic voltammograms of 0.5 mM TphP oxidation. The model for these simulations was EC, with $n = 1$, uncompensated resistance $\sim 442 \Omega$, $C_{dl} = 4 \times 10^{-7} \text{ F}$, $E^{\circ} = +1.33 \text{ V vs. SCE}$, with a homogeneous forward rate constant, $k_f = 10 \text{ s}^{-1}$, $K_{eq} = 1$ and a heterogeneous rate constant, $k^0 = 10000 \text{ cm/s}$, $\alpha = 0.5$, $D = 6.69 \times 10^{-6} \text{ cm}^2$.

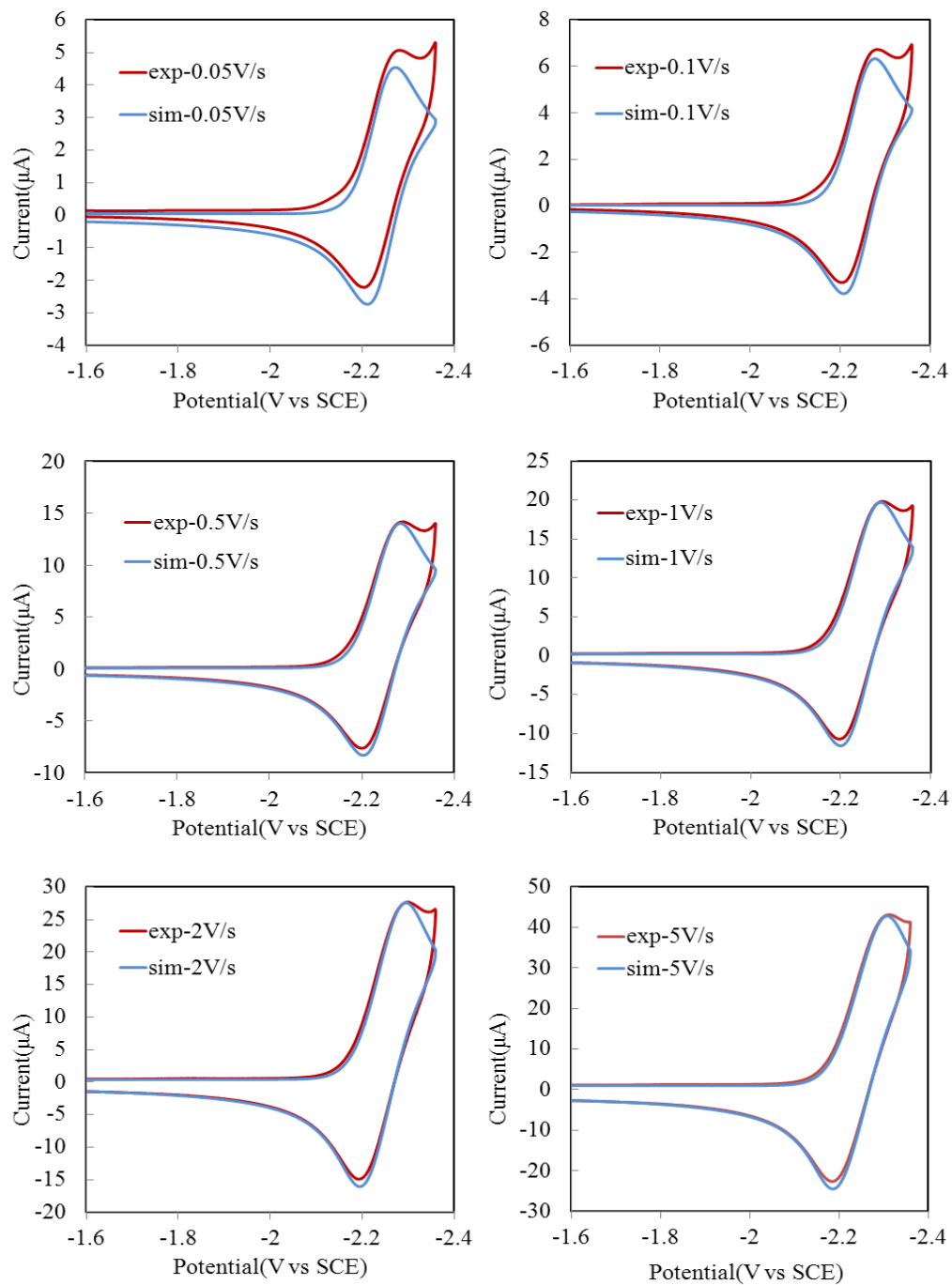


Figure S7. Experimental (red line) and simulated (blue line) cyclic voltammograms of 0.5 mM TnaP reduction. The model for these simulations was E, with $n = 1$, uncompensated resistance $\sim 560 \Omega$, $C_{dl} = 2.0 \times 10^{-7} \text{ F}$, $E^0 = -2.24 \text{ V vs. SCE}$, $k^0 = 0.2 \text{ cm/s}$, $\alpha = 0.5$, $D = 5.9 \times 10^{-6} \text{ cm}^2$.

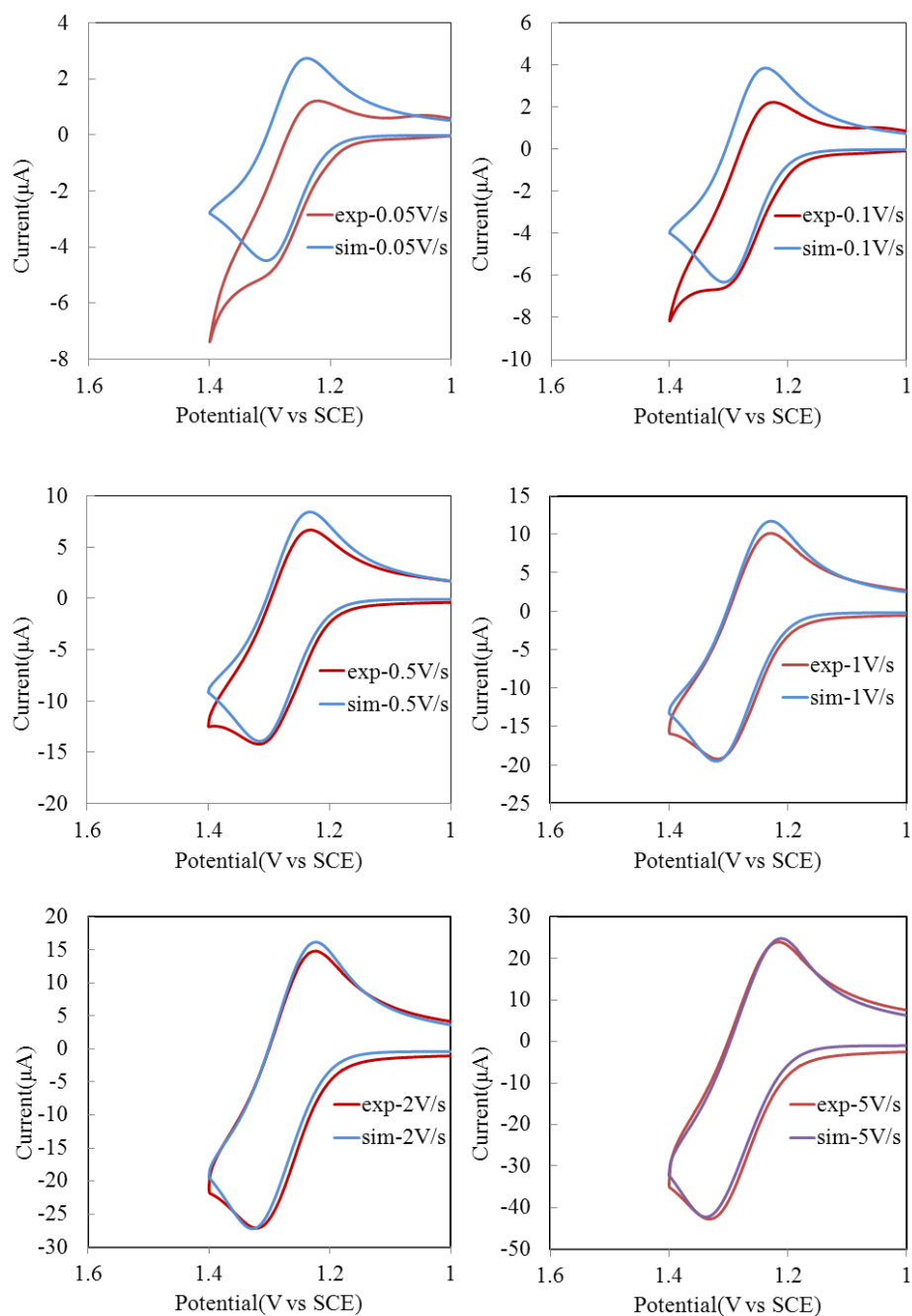


Figure S8. Experimental (red line) and simulated (blue line) cyclic voltammograms of 0.5 mM TnaP oxidation. The model for these simulations was E, with $n = 1$, uncompensated resistance $\sim 560 \Omega$, $C_{dl} = 2.0 \times 10^{-7} \text{ F}$, $E^{\circ} = +1.28 \text{ V vs. SCE}$, $k^{\circ} = 0.1 \text{ cm/s}$, $\alpha = 0.5$, $D = 5.9 \times 10^{-6} \text{ cm}^2$.

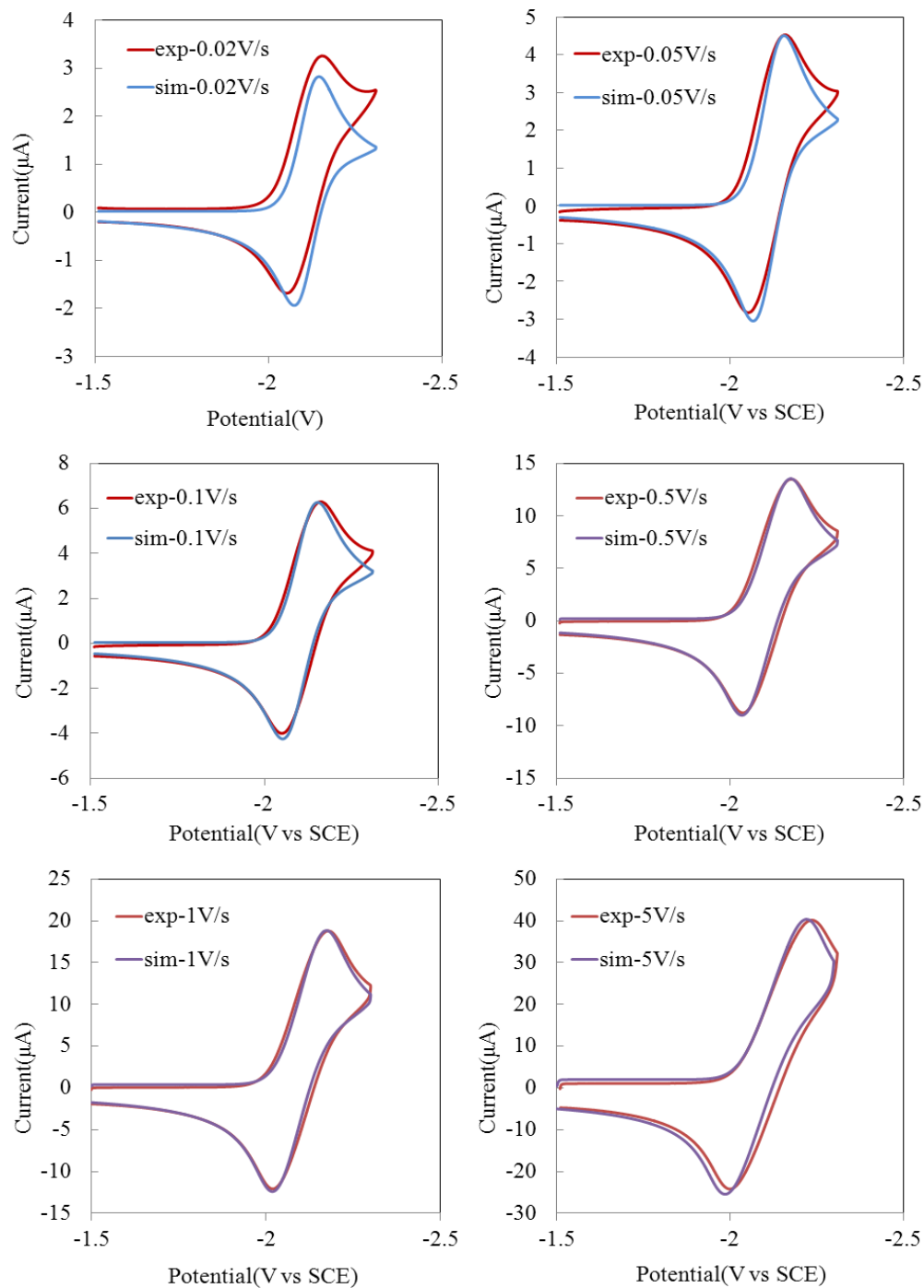


Figure S9. Experimental (red line) and simulated (blue line) cyclic voltammograms of 0.8 mM TpyP reduction. The model for these simulations was E, with $n = 1$, uncompensated resistance $\sim 1641 \Omega$, $C_{dl} = 1.06 \times 10^{-6} \text{ F}$, $E^0 = -2.10 \text{ V vs. SCE}$, $k^0 = 0.05 \text{ cm/s}$, $\alpha = 0.5$, $D = 4.74 \times 10^{-6} \text{ cm}^2$.

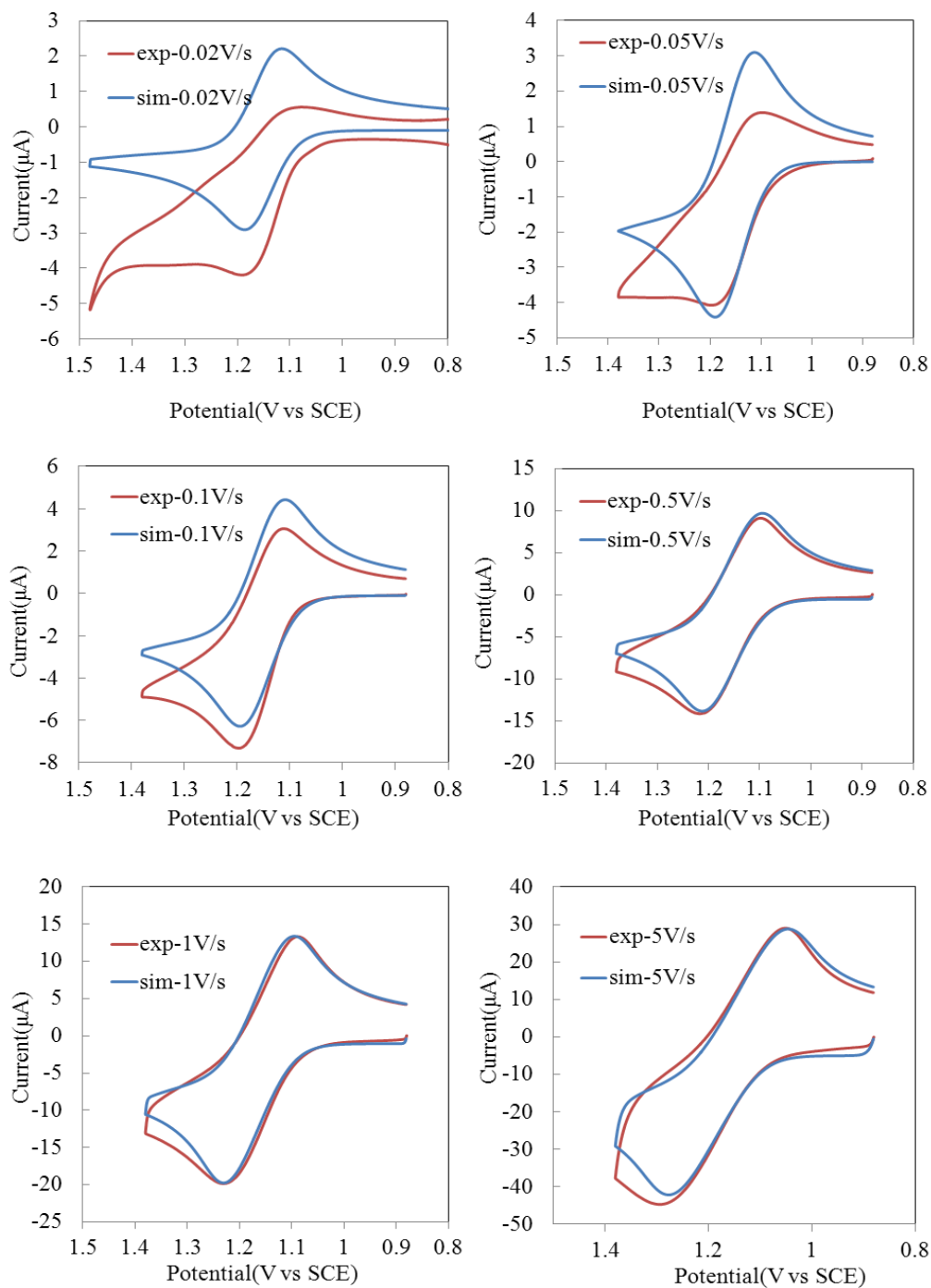


Figure S10. Experimental (red line) and simulated (blue line) cyclic voltammograms of 0.8 mM TpyP oxidation. The model for these simulations was E, with $n = 1$, uncompensated resistance $\sim 1641 \Omega$, $C_{dl} = 1.06 \times 10^{-6} \text{ F}$, $E^0 = +1.16 \text{ V vs. SCE}$, $k^0 = 0.2 \text{ cm/s}$, $\alpha = 0.5$, $D = 4.74 \times 10^{-6} \text{ cm}^2$.

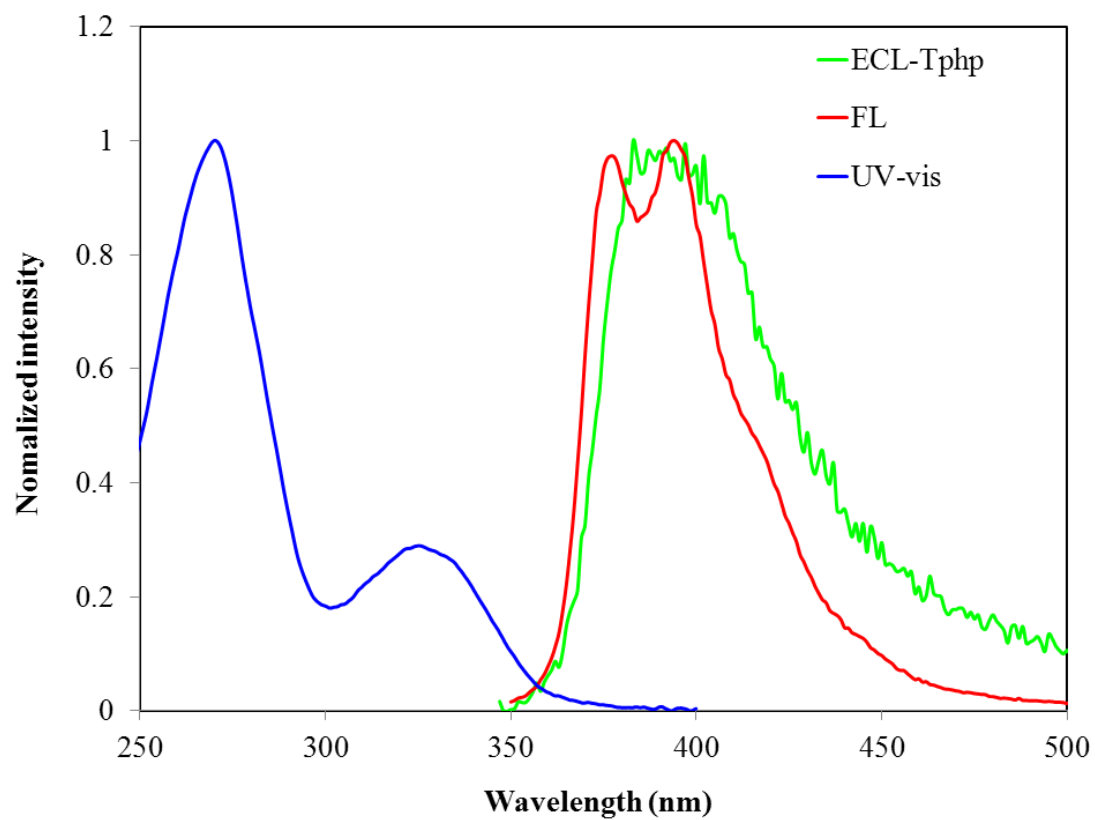


Figure S11. Normalized UV-vis (blue), fluorescence (red) and ECL (green) spectra of TphP in MeCN:Bz ($v:v=1:1$) solution; ECL conditions were the same as in Figure 5. Slit width is 1 nm for fluorescence and 20 nm for ECL spectrum.

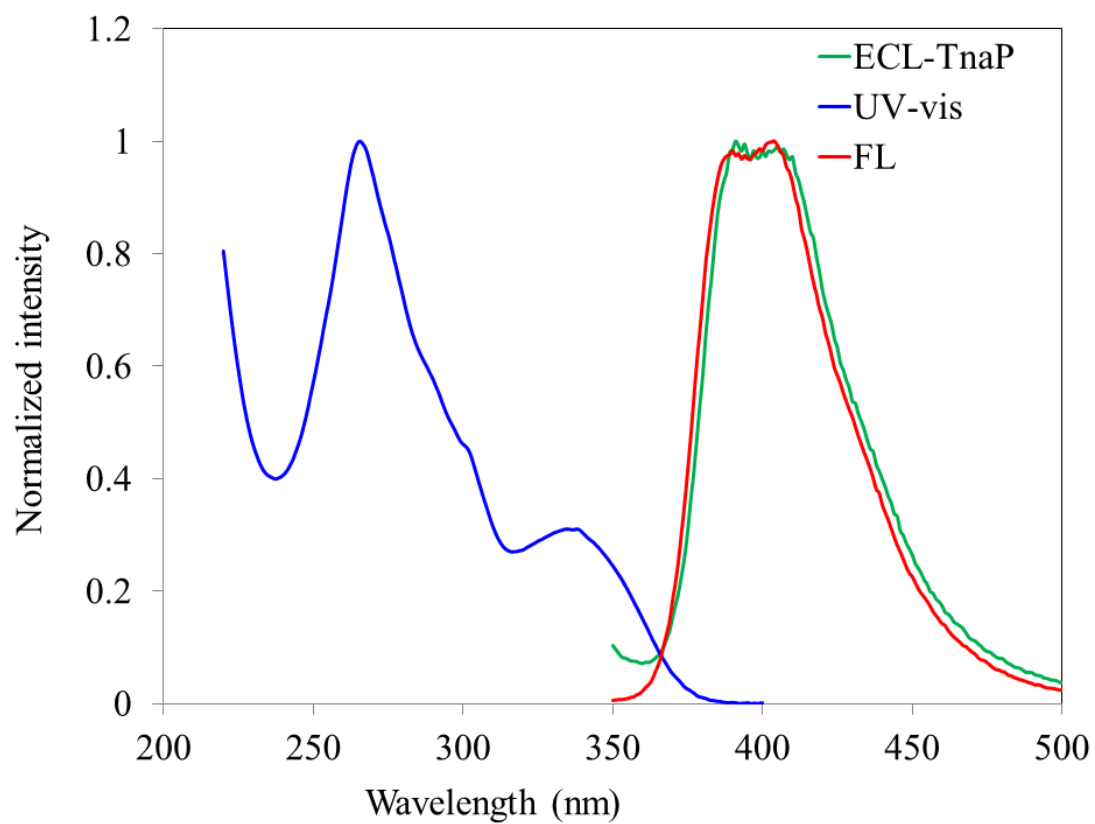


Figure S12. Normalized UV-vis (blue), fluorescence (red) and ECL (green) spectra of TnaP.

ECL conditions were the same as in Figure S11.

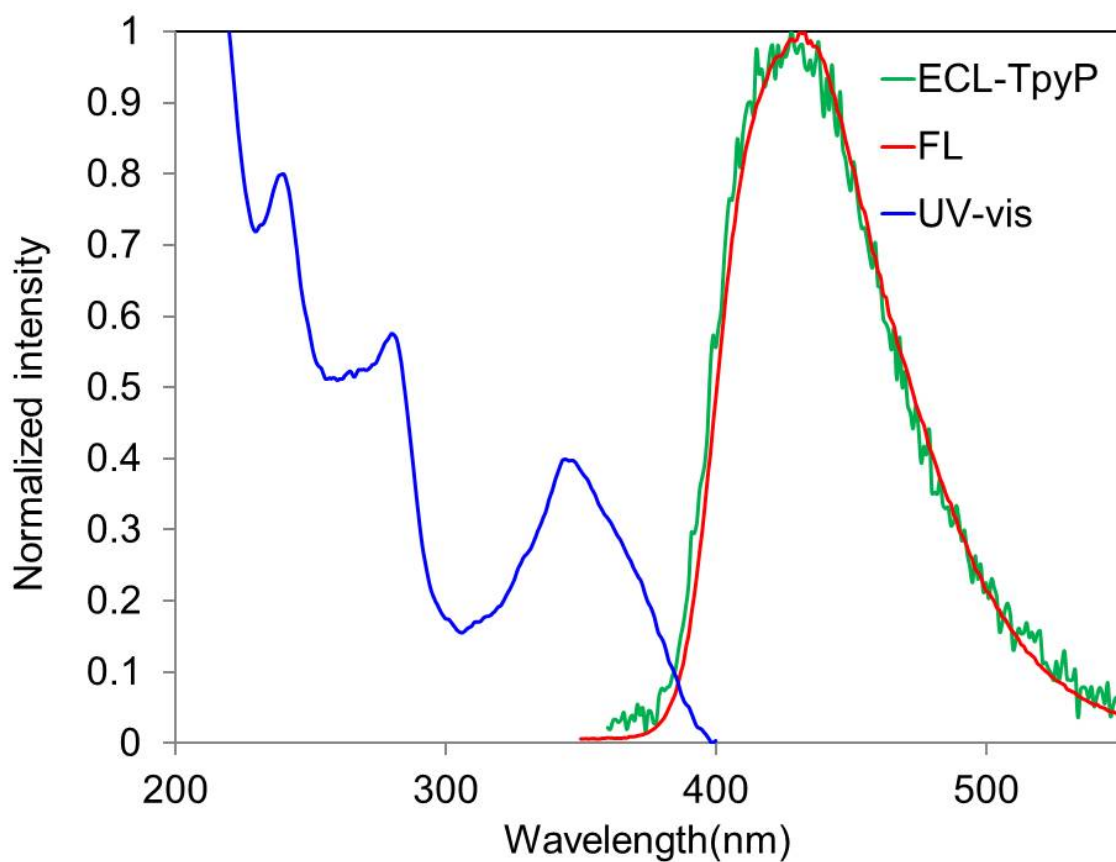


Figure S13. Normalized UV-vis absorbance (blue), fluorescence (red) and ECL (green) spectra of TpyP. Slit width is 1 nm for fluorescence and 20 nm for ECL. ECL conditions were the same as in Figure S11.

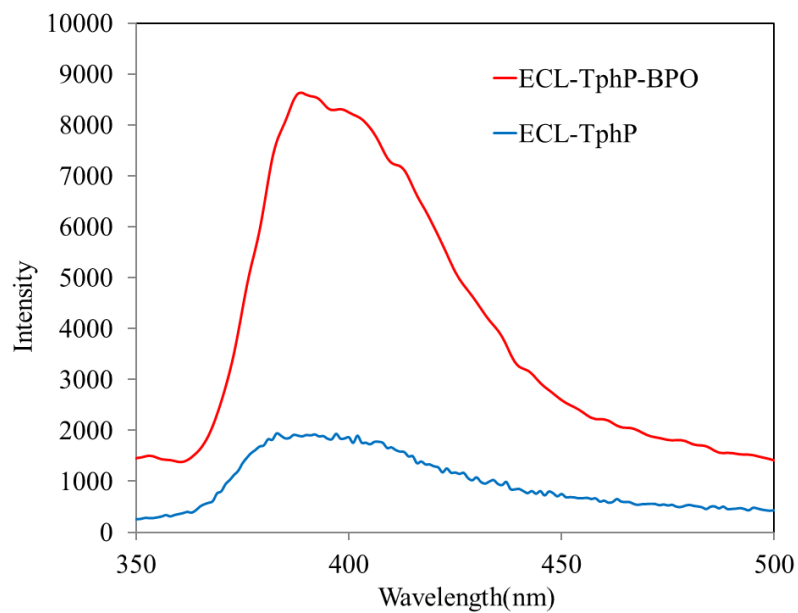


Figure S14. ECL spectra of TphP in the absence (blue) and presence (red) of BPO. Slit width is 20 nm for ECL. ECL conditions were the same as in Figure S11.

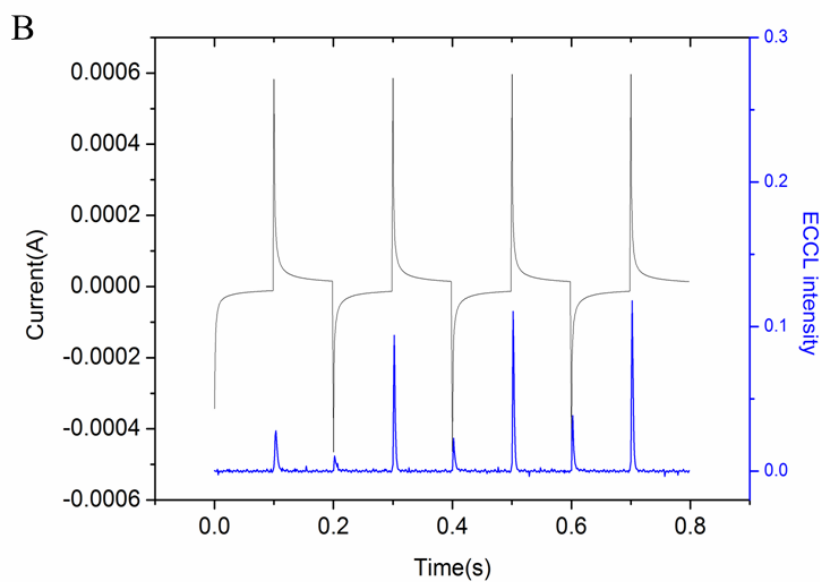
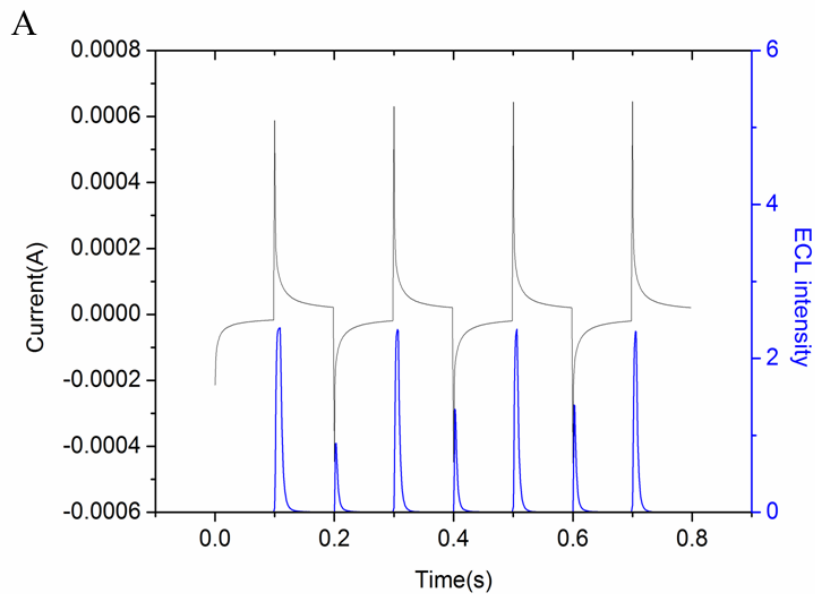


Figure S15. Initial current (black) and ECL light (blue) transients for 0.5 mM TnaP (A) and 0.8 mM TpyP (B) pulsed between 80 mV past the first reduction peak and at 80 mV past the first oxidation potential, respectively. Pulse width is 0.1 s.

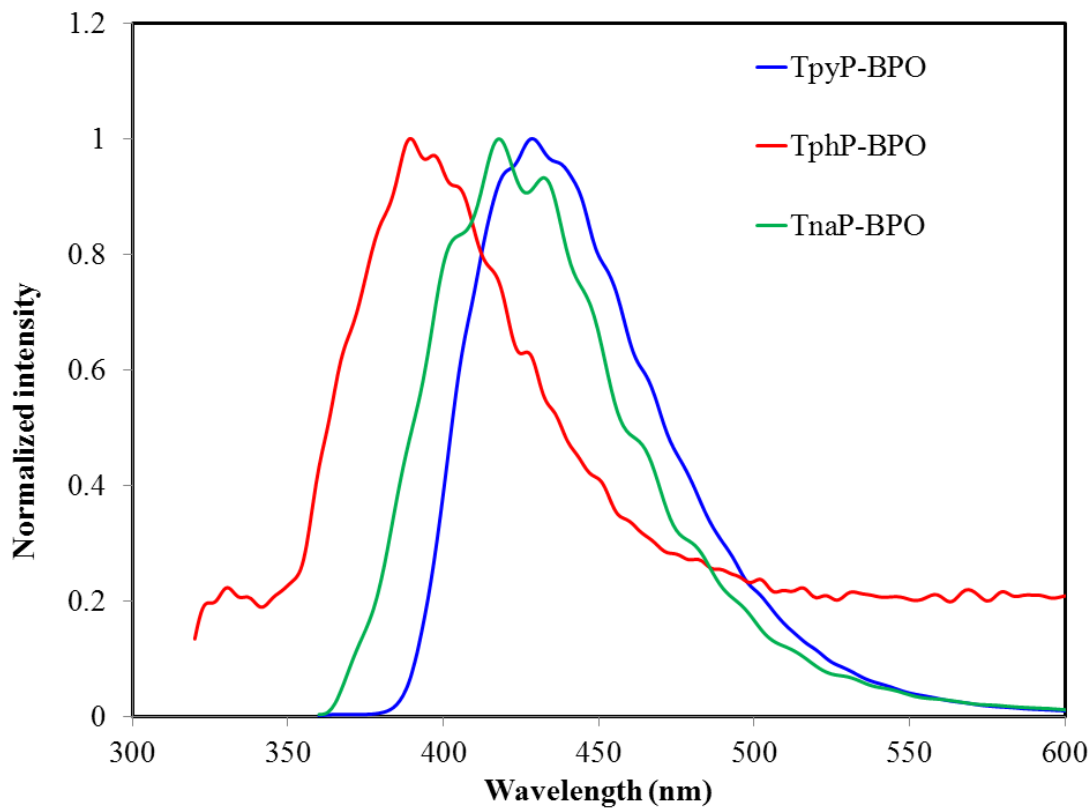


Figure S16. Normalized ECL spectra of TphP-BPO (red), TnaP-BPO (green) and TpyP-BPO (blue). Slit width is 20 nm. ECL conditions were pulsed between 80 mV past the first reduction peak and 0. Pulse width is 0.1 s.